

Measurement of acoustic dissipation occurring in narrow channels with wet wall

Yuki Ueda^{1, a)} and Naoyuki Ogura¹

Department of Bio-Functions and Systems Science, Tokyo

University of Agriculture and Technology, Koganei, Tokyo 184-8588,

Japan

1 The acoustic dissipation that occurs in a porous medium is experimentally investi-
2 gated. Two conditions are tested. One is that the wall of the porous medium is wet
3 by water, and the other is that it is dry. Experimental results show that water does
4 not affect viscous dissipation; however, it affects the dissipation caused by pressure
5 oscillation. Furthermore, it is found that the effect of water on the dissipation due
6 to pressure oscillation increases with the temperature of the working gas. A theory
7 that can consider the effect of condensation and evaporation on sound propagation is
8 used to investigate the result. The theoretically and experimentally obtained values
9 of dissipation are in good agreement. The reason for the effect of water is analyzed
10 using the theory.

^{a)}uedayuki@cc.tuat.ac.jp

11 **I. INTRODUCTION**

12 Acoustic wave propagation in a gas-filled tube is a classical problem in fluid dynamics.
13 Several researchers, such as Helmholtz, Kirchhoff, and Rayleigh, have derived theories to
14 describe this phenomenon. (See the literatures listed in the paper¹.) Tijdeman used the
15 limit conditions that are suitable for treating engineering acoustics and obtained a simple
16 expression for acoustic propagation. Yazaki et al. measured the propagation constant in a
17 cylindrical tube, and their results were in good agreement with theoretical values.²

18 A few experimental studies show the effect of the condensation and evaporation of a
19 working gas on acoustic propagation. For example, Pandit and King measured the sound
20 speed in sandstone and showed that the sound speed decreases by 20–30% when relative
21 humidity is increased to 98%.³ Experimental results have motivated researchers to derivate
22 advanced acoustic theories.^{4–8} In these theories, an acoustic wave propagating in a cylindrical
23 tube is considered. However, complex channels, such as the interior of sandstone,³ are used
24 in experiments. This implies that there are extremely few experimental results that can be
25 qualitatively compared with theoretical results.

26 In this study, we have measured acoustic power dissipation in a porous medium with
27 uniform narrow channels. The measurements are performed under two conditions. One is
28 that the wall of the porous medium is wet, and the other is that it is dry. The obtained data
29 indicate that the acoustic dissipation due to velocity oscillation under the wet condition
30 is comparable to that under the dry condition. On the contrary, the acoustic dissipation
31 due to pressure oscillation under the wet condition is larger than that under the dry condi-

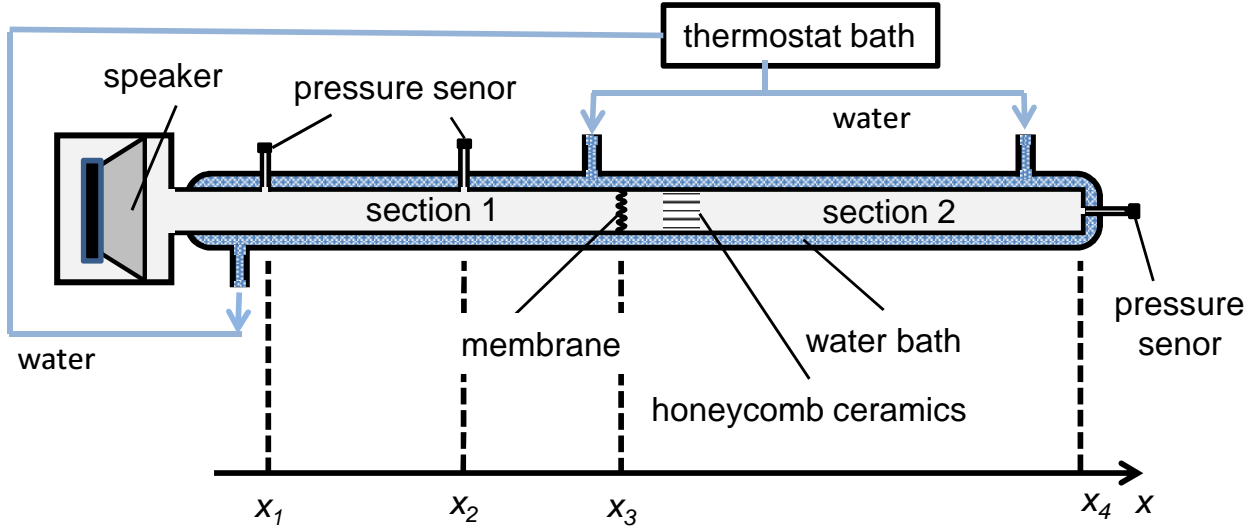


FIG. 1. Schematic illustration of the experimental setup.

32 tion. Experimental results are compared with the numerical results obtained based on the
 33 theory⁵⁻⁷ proposed by Raspet et al., and good agreement is obtained between the results.

34 The rest of this paper is organized as follows: Sections II and III describe the experimental
 35 setup and measurement method, respectively. Section IV presents experimental results, and
 36 Sec. V shows their comparison with theoretical results. The results are summarized in Sec.
 37 VI.

38 II. EXPERIMENTAL SETUP

39 Figure 1 shows the schematic illustration of the constructed experimental setup. It es-
 40 sentially comprises three components, i.e., an acoustic driver (speaker), a water bath, and a
 41 resonator. The acoustic driver [Fostex model FW160N] is electronically connected to a sig-
 42 nal generator [Tektronix model AFG1062] via an audio amplifier [Yamaha model P2500S],
 43 and it inputs an acoustic wave to the resonator. The internal diameter of the resonator is 40

Measurement of acoustic dissipation occurring in narrow channels with wet wall

44 mm, and its length is approximately 2.2 m. The resonator is covered by the water bath to
45 eliminate thermoacoustic effects⁹⁻¹² and to control the temperature (T_{gas}) of the gas inside
46 the resonator; T_{gas} is controlled between 30°C and 75°C by changing the temperature of
47 the hot water flowing in the water bath. The temperature (T_{gas}) is measured using ther-
48 mocouples installed in the resonator, which are not shown in Fig. 1. The frequency of the
49 input acoustic wave is set as 145 Hz, which is approximately the frequency of the second
50 mode in the resonator. This implies that the amplitude of oscillatory pressure becomes the
51 maximum close to the center of the resonator, whereas the amplitude of oscillatory velocity
52 becomes the minimum close to the center.

53 The space in the resonator is divided into two parts (section 1 and section2) by an elastic
54 membrane. This realizes the following two conditions: The first is that the acoustic wave
55 travels through the entire space in the resonator. This is because the acoustic wave passes
56 through the membrane. The second is that the working fluids in the two sections do not
57 mix. The working gas in section 1 is room air whose absolute humidity is lower than 12
58 g/m³. The effect of the membrane on the measurements is discussed in Sec. III A.

59 A ceramic honeycomb is inserted in section 2 (see Fig. 1), and the distance between the
60 closed end of the resonator and the ceramic honeycomb, L_{CH} , is 0.59 m or 1.13 m. The
61 reasons for this are straightforward. First, a ceramic honeycomb can easily contain water
62 on its wall. Second, it consists of numerous narrow channels, and hence, the acoustically
63 dissipated power inside it is larger than that outside it. As a result of this, the effect of
64 water can be investigated. Finally, the use of a ceramic honeycomb enables us to classify
65 dissipation into two types, i.e., the acoustic power dissipation caused by pressure oscillation

Measurement of acoustic dissipation occurring in narrow channels with wet wall

66 and that caused by velocity oscillation. The pressure-oscillation-based dissipation becomes
67 dominant when a ceramic honeycomb is located at the position ($L_{CH} = 1.13$ m) close to
68 a pressure antinode, whereas the velocity-oscillation-based dissipation becomes dominant
69 when it is located at the position ($L_{CH} = 0.59$ m) close to a velocity antinode.

70 The cross section of the channels of the used ceramic honeycomb is square. Half the
71 length of one side of the square cross section is 0.47 mm. The ceramic honeycomb is dipped
72 into water to wet the surface of its wall. The water contained in the ceramic honeycomb is
73 controlled to be 5.0 ± 0.1 g.

74 A humidity meter (Toplas Engineering model TA50) is temporally installed into section
75 2, and the humidity is checked with changing T_{gas} . It is found that the relative humidity
76 in section 2 increases owing to the water contained in the ceramic honeycomb and depends
77 on the position. The relative humidity measured close to the ceramic honeycomb and close
78 to the closed end were 90~100% and approximately 80%, respectively, when T_{gas} is higher
79 than 50°C. Note that the mean pressure inside the resonator is maintained at atmospheric
80 pressure, independent of T_{gas} .

81 To measure oscillatory pressure, three pressure sensors [Jtekt model PD104] are set on
82 the wall of the setup (see Fig. 1) via a small diameter tube whose internal diameter is 1 mm
83 and length is 25 mm. The effect of this tube on pressure measurements is examined,¹³ and
84 the correction for this effect is performed.

85 **III. METHOD OF EVALUATING ACOUSTIC DISSIPATION**

86 As shown in Fig. 1, acoustic pressure oscillation is measured at two points on the wall
 87 of section 1. The theory used to evaluate the power dissipated in section 2, W_2 , using the
 88 two measured values of pressure is described below.

89 A few expressions are used to describe acoustic wave propagation in a tube. Rott's for-
 90 mula, which is frequently used for analyzing thermoacoustic devices, is used in this study.¹⁴
 91 When the x axis is defined along a tube, the momentum and continuity equations^{14,15} of
 92 Rott's formula can be written as

$$\frac{dP}{dx} = -\frac{i\omega\rho_m}{1 - \chi_\nu}U \quad (1)$$

$$\frac{dU}{dx} = -\frac{i\omega[1 + (\gamma - 1)\chi_\alpha]}{\gamma P_m}P. \quad (2)$$

93 Here, P and U are the acoustic-oscillatory pressure and velocity, respectively; ω is angular
 94 frequency; ρ_m , P_m , γ , and σ are the mean density, mean pressure, ratio of specific heats,
 95 and Prandtl number of the working gas, respectively; χ_α and χ_ν are complex functions¹⁴⁻¹⁶,
 96 which are mentioned below. Note that U is the cross-sectional mean value and P and U
 97 are complex values. For the case of a circular-cross section tube, the functions, χ_α and χ_ν ,
 98 depend on

$$Y_\alpha = (i - 1)\sqrt{\omega\tau_\alpha} \quad (3a)$$

$$Y_\nu = (i - 1)\sqrt{\omega\tau_\nu}, \quad (3b)$$

99 and they can be expressed as¹⁴⁻¹⁶

$$\chi_\alpha = \frac{2J_1(Y_\alpha)}{Y_\alpha J_0(Y_\alpha)} \quad (4a)$$

$$\chi_\nu = \frac{2J_1(Y_\nu)}{Y_\nu J_0(Y_\nu)}, \quad (4b)$$

100 where τ_α and τ_ν are the thermal relaxation time and viscous relaxation time, respectively.¹⁶

101 They are defined as

$$\tau_\alpha = r^2/(2\alpha) \quad (5a)$$

$$\tau_\nu = r^2/(2\nu), \quad (5b)$$

102 where r is the tube radius, α is the thermal diffusivity of the working gas, and ν is its
103 kinematic viscosity.

104 Equations (1) and (2) can be solved analytically. Using the solution, the pressure and
105 cross-sectional mean velocity at $x = x_b$ can be expressed in terms of those at $x = x_a$ as¹⁷

$$\begin{pmatrix} P(x_b) \\ U(x_b) \end{pmatrix} = M(x_a, x_b) \begin{pmatrix} P(x_a) \\ U(x_a) \end{pmatrix} \quad (6)$$

106

$$M(x_a, x_b) \equiv \begin{pmatrix} m_{11}(x_a, x_b) & m_{12}(x_a, x_b) \\ m_{21}(x_a, x_b) & m_{22}(x_a, x_b) \end{pmatrix}$$

$$m_{11}(x_a, x_b) = \cos(k(x_b - x_a))$$

$$m_{12}(x_a, x_b) = -iZ_0 \sin(k(x_b - x_a))$$

$$m_{21}(x_a, x_b) = \frac{-i}{Z_0} \sin(k(x_b - x_a))$$

$$m_{22}(x_a, x_b) = \cos(k(x_b - x_a)).$$

107 Here, k and Z_0 are the complex wave number and characteristic impedance, respectively,
 108 and they are calculated as

$$k = \frac{\omega}{c} \sqrt{\frac{1 + (\gamma - 1) \chi_\alpha}{1 - \chi_\nu}}, \quad (7)$$

109 and

$$Z_0 = \rho_m \frac{\omega}{k(1 - \chi_\nu)}, \quad (8)$$

110 where c is the adiabatic sound speed.

111 The measurement points are set as x_1 and x_2 , and the point just before the elastic
 112 membrane is set as x_3 , as shown in Fig. 1. From Eq. (6),

$$U(x_1) = \frac{P(x_2) - m_{11}(x_1, x_2)P(x_1)}{m_{12}(x_1, x_2)} \quad (9)$$

113 is obtained. Equation (6) can be changed to be

$$\begin{pmatrix} P(x_3) \\ U(x_3) \end{pmatrix} = M(x_1, x_3) \begin{pmatrix} P(x_1) \\ U(x_1) \end{pmatrix}, \quad (10)$$

114 and hence,

$$\begin{aligned} \begin{pmatrix} P(x_3) \\ U(x_3) \end{pmatrix} &= M(x_1, x_3) \begin{pmatrix} P(x_1) \\ \frac{P(x_2) - m_{11}(x_1, x_2)P(x_1)}{m_{12}(x_1, x_2)} \end{pmatrix} \\ &= M(x_1, x_3) \begin{pmatrix} 1 & 0 \\ \frac{-m_{11}(x_1, x_2)}{m_{12}(x_1, x_2)} & \frac{1}{m_{12}(x_1, x_2)} \end{pmatrix} \begin{pmatrix} P(x_1) \\ P(x_2) \end{pmatrix} \end{aligned} \quad (11)$$

115 is obtained. Therefore, the simultaneous measurement of $P(x_1)$ and $P(x_2)$ yields $P(x_3)$ and
 116 $U(x_3)$.

117 Acoustic power, which is the time averaged rate of acoustic energy transmission through
 118 a cross section of the tube, is defined as

$$\begin{aligned} W(x) &= \frac{\omega S}{2\pi} \oint \operatorname{Re}[P(x)]\operatorname{Re}[U(x)]dt \\ &= \frac{S}{2} \operatorname{Re} \left[P(x)\tilde{U}(x) \right], \end{aligned} \quad (12)$$

119 where notation $\tilde{}$ indicates the complex conjugate, and S is the cross-sectional area of the
 120 tube. The acoustic power at $x = x_3$, $W(x_3)$, is obtained using $P(x_3)$, $U(x_3)$, and Eq. (12).

121 The amount of acoustic power dissipated in section 2, W_2 , can be expressed as

$$W_2 = W(x_3) - \delta W_m, \quad (13)$$

122 where δW_m is the power dissipated by the membrane. This is because the acoustic power
 123 at the closed end ($x = x_4$) must be zero.

124 **A. Preliminary experiment for evaluation of power dissipation due to membrane**

125 To estimate δW_m , preliminary measurements are performed with and without the mem-
 126 brane while maintaining $|P(x_4)|$ at 90 Pa. The ceramic honeycomb is dried and the room air
 127 is used as the working gas in both the sections in this preliminary experiment. The power
 128 dissipation δW_m can be estimated as

$$W(x_3) - W'(x_3) = \delta W_m, \quad (14)$$

129 where $W(x_3)$ and $W'(x_3)$ represent the power measured with and without the membrane,
 130 respectively. Note that the estimation of W through Eq. (6) requires the values of the gas
 131 properties. The properties of dry air are used because the “absolute” humidity of the room
 132 air is low ($< 12 \text{ g/m}^3$).

133 The measured values of $W(x_3)$, $W'(x_3)$, and δW_m are shown in Fig. 2 as a function of
 134 T_{gas} , which is varied in the next experiment. The measurements are performed using the
 135 two different honeycomb ceramic positions, i.e., $L_{CH} = 0.59$ m and $L_{CH} = 1.13$ m. The first
 136 position implies that the ceramic honeycomb exists close to the velocity antinode, whereas
 137 the second position implies that it is close to the pressure antinode. As seen from Fig. 2,
 138 the dissipation in the membrane is considerably smaller than the dissipation in section 2.
 139 The ratio $\delta W_m/W'(x_3)$ is less than 0.15 and 0.05 when $L_{CH} = 1.13$ m and $L_{CH} = 0.59$
 140 m, respectively. Moreover, it is found that δW_m changes as T_{gas} increases. This can be
 141 attributed to the fact that the increase in T_{gas} results in increase in the wavelength of the
 142 input acoustic wave through increase in sound speed. The increase in wavelength shifts
 143 the relative position of the membrane to the velocity (pressure) antinode, and then, the
 144 velocity amplitude at the membrane changes. As δW_m would depend on velocity amplitude,
 145 the measured δW_m depends on T_{gas} . These values of δW_m are considered in the analysis
 146 described in the next section.

147 IV. EXPERIMENTAL RESULTS

148 The acoustic power dissipated in section 2, W_2^{wet} , is measured by inserting the ceramic
 149 honeycomb containing 5 g water into section 2. As the maximum containable amount of
 150 water vapor in air increases with temperature of air and anomalous sound propagation was
 151 observed close to the dew point,¹⁸ T_{gas} is selected as a controlling parameter.

152 The experimental results for the case where the ceramic honeycomb is located close to
 153 the velocity antinode ($L_{CH} = 0.59$ m) are shown in Fig. 3 by closed circles, where W_2^{wet}

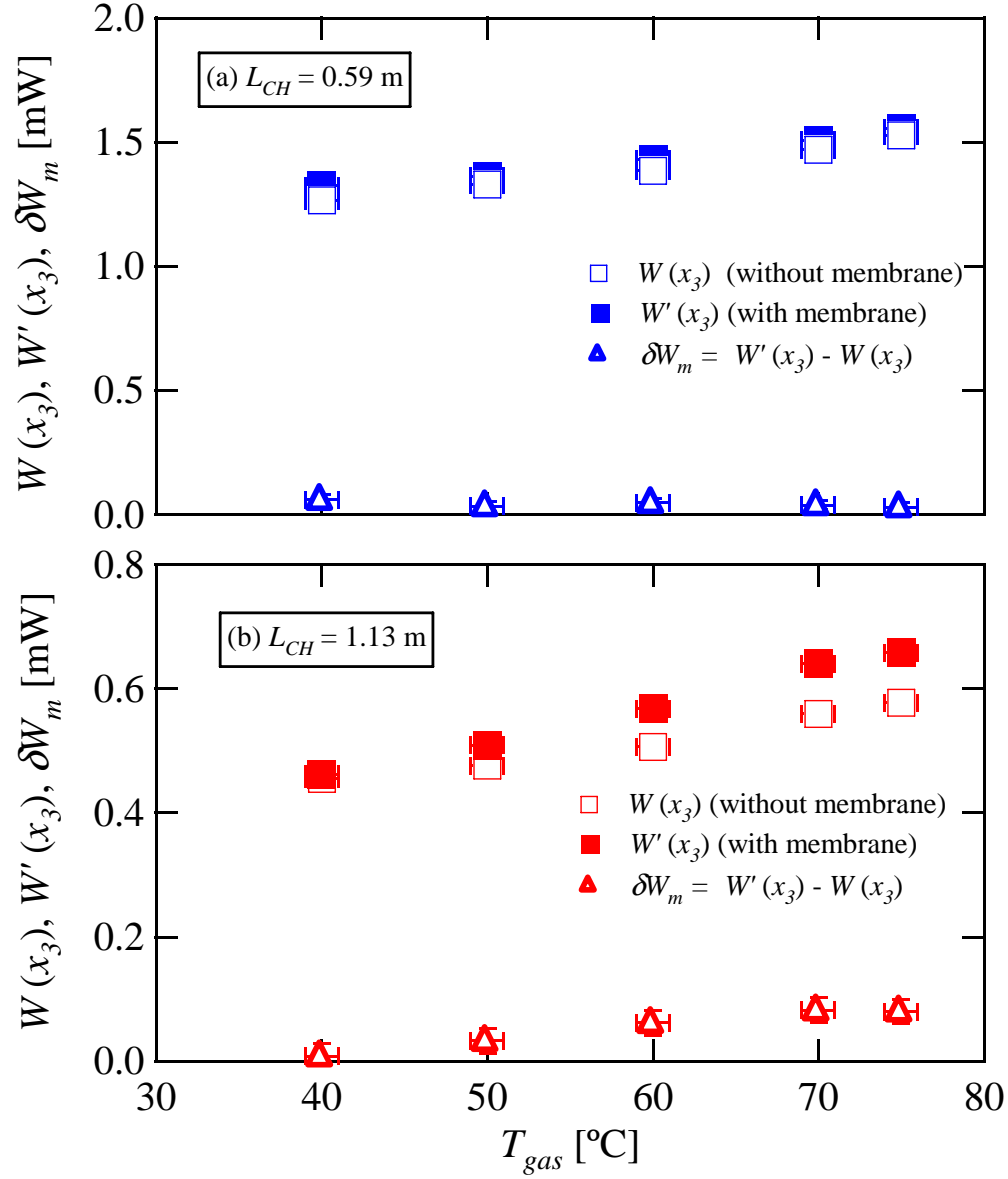


FIG. 2. Result of the preliminary experiment. The acoustic power measured close to the center of the resonator with and without the membrane is shown as a function of T_{gas} by squares and the estimated dissipation due to the membrane is shown by triangles. The data were obtained (a) when the ceramic honeycomb was located close to the velocity antinode ($L_{CH} = 0.59$ m) and (b) when the ceramic honeycomb was located close to the pressure antinode ($L_{CH} = 1.13$ m).

Measurement of acoustic dissipation occurring in narrow channels with wet wall

154 is normalized by the W_2 measured with the dried ceramic honeycomb, W_2^{dry} . As seen
155 from the figure, W_2^{wet}/W_2^{dry} does not depend on T_{gas} and its value is close to unity ($1.05 <$
156 $W_2^{wet}/W_2^{dry} < 1.09$). This indicates that the water contained in the ceramic honeycomb does
157 not strongly affect the dissipation caused by velocity oscillation, namely, viscous dissipation.
158 It should be noted that the formation of a water film on the wall of the ceramic honeycomb
159 cannot be visually observed, and hence, the flow channel radius in the ceramic honeycomb
160 would not be changed significantly by 5 g of added water.

161 Next, let us discuss the W_2^{wet}/W_2^{dry} measured under the condition that the wet ceramic
162 honeycomb is located close to the pressure antinode ($L_{CH} = 1.13$ m). As clearly shown
163 in Fig. 3 by open circles, W_2^{wet}/W_2^{dry} increases with T_{gas} and reaches 1.7 at $T_{gas}=75^\circ\text{C}$.
164 This implies that the water contained on the wall of the ceramic honeycomb contributes to
165 acoustic dissipation even when T_{gas} is below the boiling point and that the impact of the
166 water increases when T_{gas} increases to the boiling point.

167 The experimental results show that the water contained on the wall of the ceramic honey-
168 comb increases the dissipation caused by pressure oscillation, whereas the water has a small
169 impact on the dissipation due to velocity oscillation. As pressure oscillation is accompanied
170 by the oscillation of thermodynamic state properties such as temperature, it can cause the
171 condensation and evaporation of water when there is a source of water. On the contrary,
172 velocity oscillation does not directly yield the change in thermodynamic state properties.
173 Therefore, the experimental results imply that evaporation and condensation play a key role
174 in acoustic dissipation.

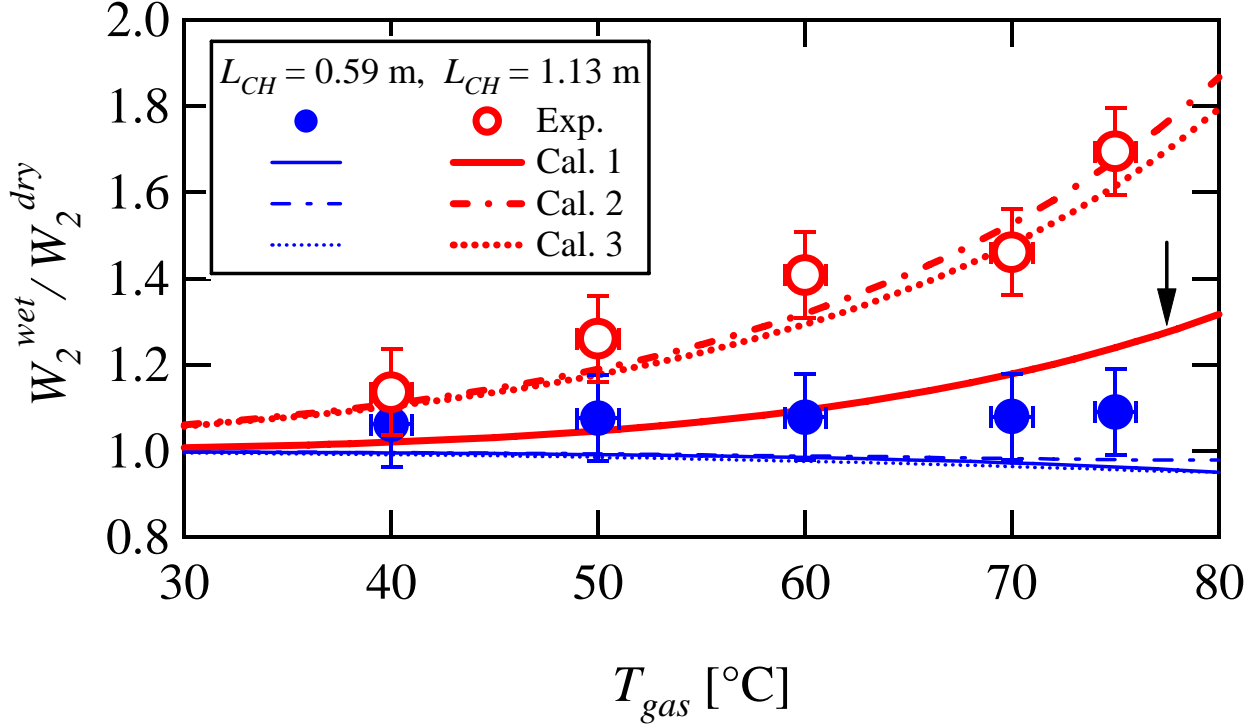


FIG. 3. Dissipation ratio as a function of gas temperature. The dissipation in section 2 with dry ceramic honeycomb (CH) is denoted as W_2^{dry} , whereas that with wet CH is denoted as W_2^{wet} .

Symbols show the experimental results and lines show the calculation results

175 **V. COMPARISON BETWEEN EXPERIMENTAL AND THEORETICAL RE-**
 176 **SULTS**

177 Raspet et al. theoretically investigated the effect of evaporation and condensation on
 178 acoustic wave propagation.⁵⁻⁷ They assumed a water film, whose thickness was zero, on a
 179 tube wall and considered mass transfer along the radial direction. We calculate W_2 using
 180 Raspet's and Rott's theories and compare them with the experimental results shown in Fig.
 181 3. First, the equations used in Raspet's theory are mentioned and then, the comparison is
 182 presented.

183 **A. Raspet's theory**

184 Raspet et al. extended Rott's theory to consider the effect of the water on the wall of the
 185 waveguide. Hence, the equations in Raspet's theory can be considerably similar to those in
 186 Rott's theory. The equations derived by Raspet et al. can be written as

$$\frac{dP}{dx} = -\frac{i\omega\rho_m}{1-\chi_v}U \quad (15)$$

$$\frac{dU}{dx} = -[1 + (\gamma - 1)\chi_\alpha]\frac{i\omega P}{\gamma P_m} - \left[\frac{n_w}{n_a}\gamma\chi_D\right]\frac{i\omega P}{\gamma P_m}, \quad (16)$$

187 where n_w and n_a are the number density of water vapor and the number density of air,
 188 respectively; χ_D is the third thermoacoustic function.^{5-7,19} As the cross section of the flow
 189 channels in the ceramic honeycomb is square,²⁰ χ_α , χ_ν , and χ_D become

$$\chi_j = 1 - \frac{64}{\pi^4} \sum_{m,n \text{ odd}} \frac{1}{m^2 n^2 Y_j} \quad (17)$$

190 with

$$Y_j = 1 - i\frac{\pi^2}{8\omega\tau_j}(m^2 + n^2), \quad (18)$$

191 where j is α , ν , or D . To calculate τ_α and τ_ν in Eq (5), half the length of one side of the
 192 square channel (0.47 mm) is used as r , and τ_D is defined as

$$\tau_D = r^2/(2D_{12}), \quad (19)$$

193 where D_{12} is the mutual diffusion coefficient, whose value can be obtained from the data
 194 book.²¹

195 Equation (15) is exactly equal to Eq. (1), whereas Eq. (16) differs from Eq. (2) by its
 196 second term on the right hand side, which describes the effect of mass transfer. Equation
 197 (6) can be used as the solution of Eqs. (15) and (16). However, the following equation must

198 be used instead of Eq. (7):

$$k_{wet} = \frac{\omega}{c} \sqrt{\frac{1 + (\gamma - 1) \chi_\alpha}{1 - \chi_\nu} + \frac{n_w}{n_a} \frac{\gamma \chi_D}{1 - \chi_\nu}}. \quad (20)$$

199 To prevent misunderstanding, we define the wave number evaluated using Eq. (7) as k_{dry} .

200 We should note that subscript *dry* indicates dry 'wall' and not dry air.

201 The numerical calculation requires the values of gas properties and the ratio of n_w and n_a
 202 of humid air because the absolute humidity is high in section 2, as mentioned in Sec. II. In
 203 this study, the equations²² based on the kinetic theory of gases and Dalton's law are used.
 204 Note that following the experimental condition, the sum of the partial pressures of air and
 205 water vapor is set to 101 kPa.

206 B. Comparison

207 We perform three types of calculation to verify the theory. Section 2 is divided into two
 208 parts for the calculation. One part is the interior of the ceramic honeycomb and the other is
 209 the exterior. In all calculations, the gas properties of humid air, whose relative humidity is
 210 100%, are used for the interior of the ceramic honeycomb. The relative humidity outside the
 211 ceramic honeycomb is set as 80% or 100%. This is because the relative humidity measured
 212 outside the ceramic honeycomb is over 80%. In the first calculation (Cal. 1), k_{dry} is used
 213 for the interior and exterior of the ceramic honeycomb. In the second and third calculations
 214 (Cal. 2 and Cal. 3), k_{wet} is used for the interior and k_{dry} is used for the exterior. These
 215 conditions are shown in Table I.

TABLE I. Calculation conditions. k_{dry} indicates the use of Eq. (7), whereas k_{wet} does the use of Eq. (20). RH denotes relative humidity.

	In ceramic honeycomb	Outside ceramic honeycomb
Cal. 1	k_{dry} , RH=100%	k_{dry} , RH=100%
Cal. 2	k_{wet} , RH=100%	k_{dry} , RH=100%
Cal. 3	k_{wet} , RH=100%	k_{dry} , RH=80%

216 The calculated results are shown in Fig. 3 by lines. As seen from Fig. 3, when the
 217 ceramic honeycomb is located close to the pressure antinode ($L_{CH} = 1.13$ m), the result of
 218 Cal. 1 (shown by the thick solid line indicated by an arrow in Fig. 3) is smaller than the
 219 experimental results shown by open circles. This indicates that the experimentally obtained
 220 increase in W_2^{wet}/W_2^{dry} with T_{gas} cannot be explained by only the difference between the
 221 gas properties of dry air and humid air. On the contrary, the temperature dependence
 222 of W_2^{wet}/W_2^{dry} for both cases ($L_{CH} = 1.13$ m and 0.59 m) approximately agrees with the
 223 calculated results (Cal. 2 and Cal. 3), which are shown by dotted and dot-and-dash lines.
 224 Thus, this comparison supports the theory proposed by Raspet et al.

225 Rott's and Raspet's theories can explain the experimentally obtained dependency of
 226 W_2^{wet}/W_2^{dry} on T_{gas} as follows: The dissipation of acoustic power can be written as

$$\Delta W = \int_{x_a}^{x_b} \frac{dW}{dx} dx = \int_{x_a}^{x_b} \frac{d}{dx} \left(\frac{S}{2} \text{Re} [P\tilde{U}] \right) dx. \quad (21)$$

227 When cross-sectional area S is constant,

$$\Delta W = \frac{S}{2} \int_{x_a}^{x_b} \left(\text{Re} \left[\frac{dP}{dx} \tilde{U} + \tilde{P} \frac{dU}{dx} \right] \right) dx. \quad (22)$$

228 Hence, Rott's theory (Eqs. (1) and (2)) shows

$$\Delta W = \frac{S}{2} \int_{xa}^{xb} (R_{dry}|U|^2 + K_{dry}|P|^2) dx, \quad (23)$$

229 where

$$R_{dry} = \omega \rho_m \text{Im} \left[\frac{1}{1 - \chi_\nu} \right] \quad (24)$$

$$K_{dry} = \frac{\gamma - 1}{\gamma P_m} \omega \text{Im} [\chi_\alpha]. \quad (25)$$

230 On the contrary, Raspet's theory (Eqs. (15) and (16)) gives

$$\Delta W = \frac{S}{2} \int_{xa}^{xb} (R_{wet}|U|^2 + K_{wet}|P|^2) dx, \quad (26)$$

231 where

$$R_{wet} = \omega \rho_m \text{Im} \left[\frac{1}{1 - \chi_\nu} \right] \quad (27)$$

$$K_{wet} = \frac{\gamma - 1}{\gamma P_m} \omega \text{Im} [\chi_\alpha] + \frac{n_w}{n_a} \text{Im} [\chi_D] \frac{\omega}{P_m}. \quad (28)$$

232 The first terms on the right hand side of Eqs. (23) and (26) are proportional to the square
 233 of velocity amplitude, whereas the second terms are proportional to the square of pressure
 234 amplitude. Furthermore, all of them have negative values, indicating a decrease in acoustic
 235 power. As $R_{wet} = R_{dry}$, which are relative to the first terms on the right hand side of Eqs.
 236 (23) and (26), the theories indicate that the dissipation due to velocity oscillation does not
 237 depend on the water on the wall of the flow channel. This is consistent with the experimental
 238 results. On the contrary, K_{wet} has an additional term, which is the second term of the right
 239 hand side of Eq. (28). As this term has a negative value, the theories indicate that the water
 240 on the wall affects the dissipation caused by pressure oscillation. In addition, the second
 241 term is proportional to n_w/n_a . The coefficient n_w/n_a increases as the temperature of water

242 approaches its boiling point if relative humidity is maintained at a constant value. Hence,
243 the effect of the second term increases with T_{gas} , resulting in the increase in W_2^{wet}/W_2^{dry} .
244 These results indicated by the theories are also consistent with the experimental results.

245 VI. CONCLUSION

246 The acoustic dissipation in a wet-wall porous medium was measured. The experimental
247 results indicated that the dissipation caused by acoustic velocity oscillation was not affected
248 by the water on the wall of the porous medium. On the contrary, the dissipation caused
249 by acoustic pressure oscillation was affected by water, particularly when the temperature of
250 the working gas was close to the boiling temperature of water. These results were compared
251 with the results calculated based on the theory proposed by Raspet et al.,⁵⁻⁷ and the validity
252 of the theory was demonstrated.

253 ACKNOWLEDGMENTS

254 This work was supported by JSPS KAKENHI Grant Number 17K17705.

255 REFERENCES

- 256 ¹H. Tijdeman, “On the propagation of sound waves in cylindrical tubes,” *J. Sound Vib.*
257 **39**, 1–33 (1975).
- 258 ²T. Yazaki, Y. Tashiro, and T. Biwa, “Measurements of sound propagation in narrow
259 tubes,” *Proc. R. Soc. London, Ser. A* **463**, 2855–2862 (2007).

- 260 ³B. I. Pandit and M. S. King, “The variation of elastic wave velocities and quality factor q
261 of a sandstone with moisture content,” *Can. J. Earth Sci.* **16**, 2187–2195 (1979).
- 262 ⁴Y. Mao, “Sound attenuation in a cylindrical tube due to evaporation-condensation,” *J.*
263 *Acoust. Soc. Am.* **104**, 664–670 (1998).
- 264 ⁵R. Raspet, C. Hickey, and J. Sabatier, “The effect of evaporation-condensation on sound
265 propagation in cylindrical tubes using the low reduced frequency approximation,” *J.*
266 *Acoust. Soc. Am.* **105**, 65–73 (1999).
- 267 ⁶C. Hickey, R. Raspet, and W. Slaton, “Effects of thermal diffusion on sound attenuation
268 in evaporating and condensing gas-vapor mixtures in tubes,” *J. Acoust. Soc. Am.* **107**,
269 1126–1130 (2000).
- 270 ⁷R. Raspet, W. Slaton, C. Hickey, and R. Hiller, “Theory of inert gas-condensing vapor
271 thermoacoustics: propagation equation,” *J. Acoust. Soc. Am.* **112**, 1414–1422 (2002).
- 272 ⁸C. Guianvarc’h, M. Bruneau, and R. M. Gavioso, “Acoustics and precondensation phe-
273 nomena in gas-vapor saturated mixtures,” *Phys. Rev. E* **89**, 023208 (2014).
- 274 ⁹D. Noda and Y. Ueda, “A thermoacoustic oscillator powered by vaporized water and
275 ethanol,” *Am. J. Phys.* **81**, 124–126 (2013).
- 276 ¹⁰K. Tsuda and Y. Ueda, “Abrupt reduction of the critical temperature difference of a
277 thermoacoustic engine by adding water,” *AIP Adv.* **5**, 097173 (2015).
- 278 ¹¹K. Tsuda and Y. Ueda, “Critical temperature of traveling- and standing-wave thermo-
279 acoustic engines using a wet regenerator,” *Appl. Energy* **196**, 62 – 67 (2017).

- 280 ¹²T. Biwa, Y. Tashiro, U. Mizutani, M. Kozuka, and T. Yazaki, “Experimental demon-
281 stration of thermoacoustic energy conversion in a resonator,” *Phys. Rev. E* **69**, 066304
282 (2004).
- 283 ¹³T. Biwa, Y. Ueda, T. Yazaki, and U. Mizutani, “Work flow measurements in a thermoacoustic engine,” *Cryogenics* **41**, 305–310 (2001).
- 284
- 285 ¹⁴N. Rott, “Damped and thermally driven acoustic oscillations,” *Z. Angew. Math. Phys.* **20**,
286 230–243 (1969).
- 287 ¹⁵G. W. Swift, *Thermoacoustics: A Unifying Perspective for Some Engines and Refrigerators*
288 (Acoustical Society of America, Pennsylvania, 2002).
- 289 ¹⁶A. Tominaga, *Fundamental Thermoacoustics* (Uchidarokakumo, Tokyo, 1998).
- 290 ¹⁷Y. Ueda and C. Kato, “Stability analysis for spontaneous gas oscillations thermally induced
291 in straight and looped tubes,” *J. Acoust. Soc. Am.* **124**, 851–858 (2008).
- 292 ¹⁸J. B. Mehl and M. R. Moldover, “Precondensation phenomena in acoustic measurements,”
293 *J. Chem. Phys.* **77**, 455–465 (1982).
- 294 ¹⁹W. V. Slaton, R. Raspet, C. J. Hickey, and R. A. Hiller, “Theory of inert gas-condensing
295 vapor thermoacoustics: Transport equations,” *J. Acoust. Soc. Am.* **112**, 1423–1430 (2002).
- 296 ²⁰W. Arnott, H. Bass, and R. Raspet, “General formulation of thermoacoustics for stacks
297 having arbitrarily shaped pore cross sections,” *J. Acoust. Soc. Am.* **90**, 3228–3237 (1991).
- 298 ²¹*JASM data book: Thermophysical properties of fluids* (Japan society of mechanical engi-
299 neers, Tokyo, 1983).

Measurement of acoustic dissipation occurring in narrow channels with wet wall

300 ²²S. Ooe, *Bussei Teisuu Suisan Hou (Physical property estimation methods)* (Nikkann
301 Kougyou Shinbunsha, Tokyo, 1985).